Supporting Information

Bachmann et al. 10.1073/pnas.1012668108

SI Text

SI Methods. ***Peptide synthesis and purification.*** S-peptide variants were synthesized by standard Fmoc-solid phase peptide synthesis in an Applied Biosystems 433A automated peptide synthesizer. Thioxo peptides were synthesized as described (1, 2). The raw product was purified by reversed-phase HPLC-chromatography using a C8 reversed-phase column and eluted with a water/acetonitrile gradient.

S-protein preparation. 50 mg RNase A in 1 mL 100 mM Tris/HCl pH 7.7 were digested with 40 μL subtilisin (1 mg/mL) while stirring at 4 °C overnight (18 h). The pH was subsequently lowered to 2.5 (1N HCl) for 1 h and raised again to pH 7 with 1N NH_4OH. 50 mM BICINE pH 7.6 were added to yield 4 mL of solution. To separate the cleaved product from uncleaved RNase A the sample was applied to a carboxy methyl (CM)-sepharose column equilibrated with 50 mM BICINE and eluted with a salt gradient (0.2 M sodium phosphate). Peak fractions were pooled and desalted in portions on a protein desalting (PD) 10 column. The eluate was mixed with the same volume acetic acid to yield a solution containing 50% acetic acid in order to dissociate the RNase S-complex. S-peptide was separated from S-protein by G50 gel filtration column under acetic conditions (50% acetic acid). The fractions containing S-protein were dialyzed against the measuring buffer and frozen in liquid nitrogen for storage at −80 °C.

ITC measurements. Equilibrium stability (ΔG^0) of the RNaseS complex was determined by isothermal titration calorimetry (ITC) using a Microcal VP ITC titration calorimeter. S-peptide variants at a concentration of 375 μM were titrated in 7 μL steps into S-protein solution of 25 μM concentration. S-peptide and S-protein were dialyzed against 50 mM sodium acetate (NaOAc) pH 6.0, 100 mM NaCl before the titration experiment. The data were fitted to a single-site binding model, which yields the equilibrium constant and the molar binding enthalpy.

Activity assay. The equilibrium constant for very instable complexes was determined by an activity assay (3). 2 μM S-protein was incubated with increasing amounts S-peptide. The RNase S substrate 2′,3′cCMP was added at concentrations between 0.2–0.5 mM. Cleavage was followed photometrically at 290 nm and the initial slope of the reaction was plotted against S-peptide concentration and analyzed to a single binding-site model to yield the equilibrium constant.

Kinetic measurements. Association kinetics were measured under pseudo-first-order conditions with an excess of S-peptide. Varying concentrations of S-peptide were mixed in 1 : 1 (volume : volume) mixing ratio with 5 μM S-protein under pseudo-first-order conditions in a stopped-flow apparatus. Fluorescence above 305 nm after excitation at 280 nm was recorded with an Applied Photophysics SX20 instrument. For S-peptide variants containing tyrosine, tryptophan, or naphthylalanine the excitation wavelengths were shifted to higher wavelengths to avoid the inner filter effect. Stopped-flow CD measurements were carried out in an Applied Photophysics PiStar spectropolarimeter equipped with a stopped-flow mixing unit. Changes in ellipticity were recorded at 225 nm. All kinetics were fit to single or double exponential functions. To obtain the second-order rate constant for association (k_{on}), the slope of the concentration dependence of the measured pseudo-first-order rate constants (k_{obs}) was analyzed according to

$$k_{obs} = k_{on} \cdot [\text{S-peptide}].$$

Unless otherwise stated, buffer conditions were 50 mM NaOAc, 100 mM NaCl, pH 6.0.

Equilibrium Circular Dichroism measurements. Temperature-dependence of the far-UV CD signal at 222 nm was measured to test for helix formation in the isolated S-peptide variants. Spectra were recorded between 250 and 196 nm with 2 nm bandwidth and 125 μM sample concentration in a 1 mm cell under the usual buffer conditions. For thermals transitions the sample was placed into a 1 cm cell at 12.5 μM concentration and the signal change at 222 nm was followed between 5 °C and 85 °C. The sample was allowed to equilibrate for 1 min at each temperature before measurements.

1. Wildemann D, Drewello M, Fischer G, Schutkowski M (1999) Extremely selective $Mg(ClO_4)_2$ mediated removal of Bpoc/Ddz moieties suitable for the solid phase peptide synthesis of thioxo peptides. *Chem. Commun.*: 1809–1810.
2. Wildemann D, et al. (2007) A nearly isosteric photosensitive amide-backbone substitution allows enzyme activity switching in ribonuclease S. *J Am Chem Soc* 129:4910–4918.
3. Woodfin BM, Massey V (1968) Spectrophotometric determination of the dissociation constant of ribonuclease S`. *J Biol Chem* 243:889–892.

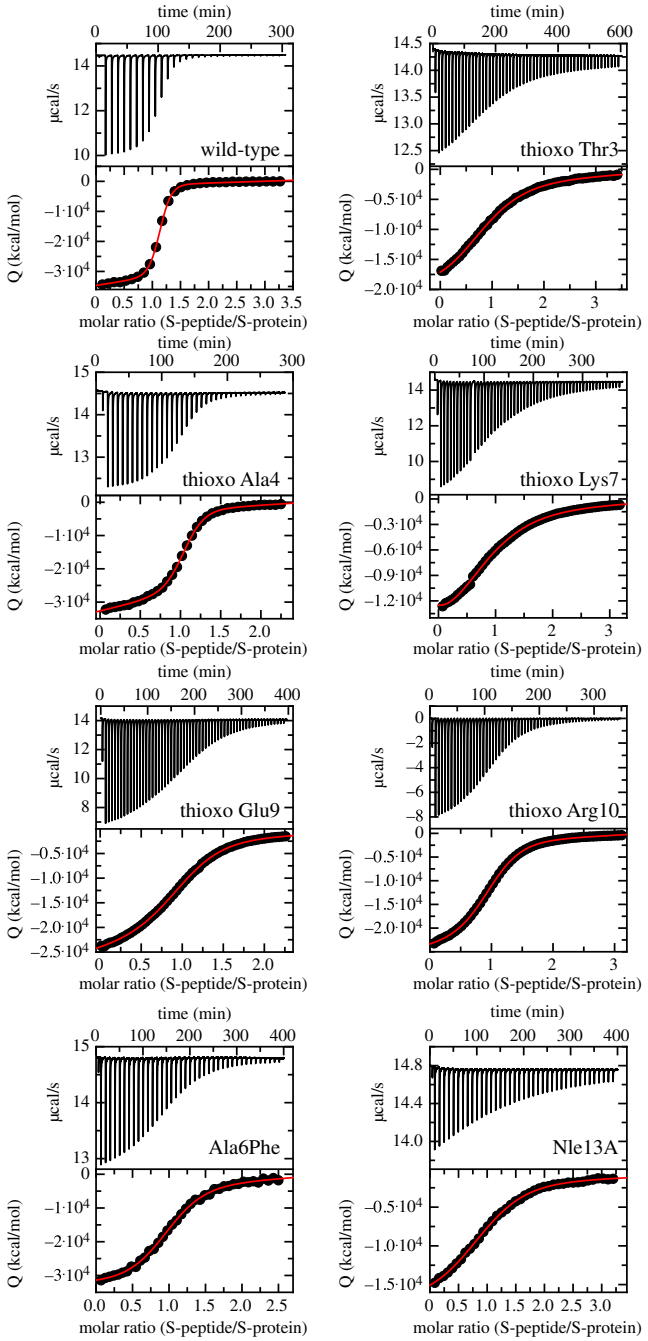

Fig. S1. Stability of the RNase S complex determined by ITC for the S-peptide variants used to calculate ϕ-values. Conditions were pH 6.0, 50 mM NaOAc, 100 mM NaCl at 25 °C. The resulting equilibrium constants (K_{eq}) are given in Tables 1 and 2.

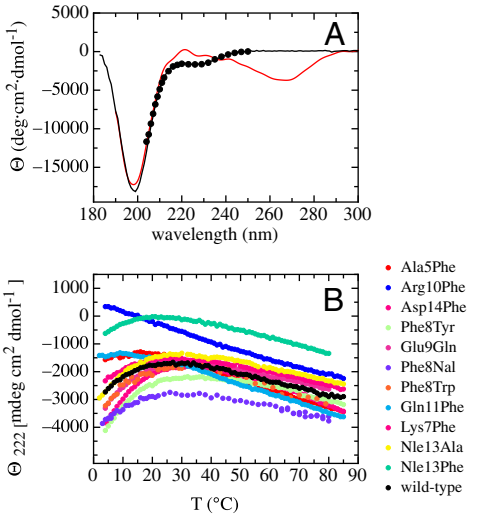

Fig. S2. (*A*) Effect thioxylation on the CD spectrum of the S-peptide at 25 °C. The spectrum of the thioxo Ala4 variant (red line) shows additional bands around 270 nm and 220 nm compared to the wild-type S-peptide (black line and solid black diamond) due to absorbance of the thioxo-peptide bond. These additional bands do not allow a quantitative comparison of oxo- and thioxo-peptides. However, the shape of the spectrum below 210 nm, indicates an unfolded conformation of both peptides. Spectra (solid lines) were taken in 10 mM sodium phosphate pH 6.0. The spectrum under conditions used for ϕ-value analysis (pH 6.0, 50 mM NaOAc, 100 mM NaCl) can not be measured below 205 nm due to the high salt concentration. It is, however, identical to the spectrum at low salt in the accessible range between 250 and 205 nm (solid black diamond) (*B*) Thermal transitions of the different S-peptide variants measured by the change in ellipticity at 222 nm. The initial increase in ellipticity observed for some variants indicates melting of small amounts of helical structure (<10%). The slight linear decrease in ellipticity with increasing temperature is typically observed for unfolded polypeptide chains. At 25 °C there is no evidence for helical structure in any of the variants. The differences in the absolute values of the CD signal is most likely due to the presence of additional Phe, Nal, Trp, or Tyr residues, which are known to have a significant contribution to the protein CD properties in the far-UV region. Conditions were pH 6.0, 50 mM NaOAc, 100 mM NaCl at 25 °C for all measurements.

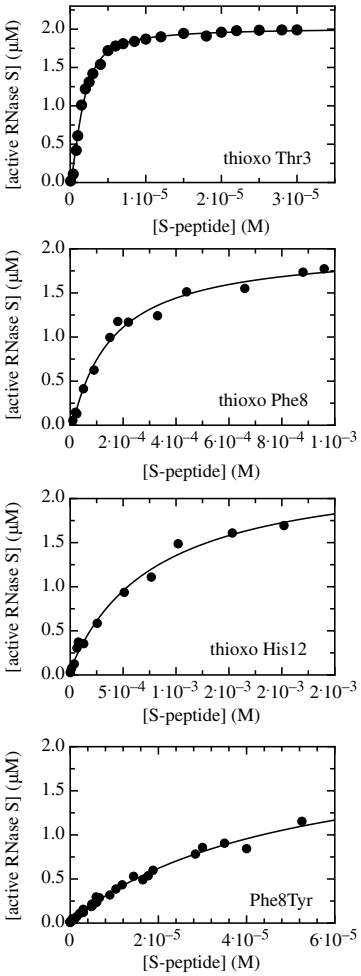

Fig. S3. Stability of the RNase S complex measured by an activity assay for S-peptide variants that show drastically reduced complex stability. Additionally, the results from the activity for the thioxo-Thr3 S-peptide variant are shown for comparison with the results from ITC measurements. The fit for this variant of the data gives $\Delta G^0 = -35.6 \pm 0.3$ kJ/mol, which is in good agreement with results from the ITC measurement ($\Delta G^0 = -35.1 \pm 0.4$ kJ/mol; see Fig. S1 and Table 1), which shows that the two methods give identical results. Conditions were pH 6.0, 50 mM NaOAc, 100 mM NaCl at 25 °C. The results of the fits to a single binding-site model are given in Tables 1 and 2.

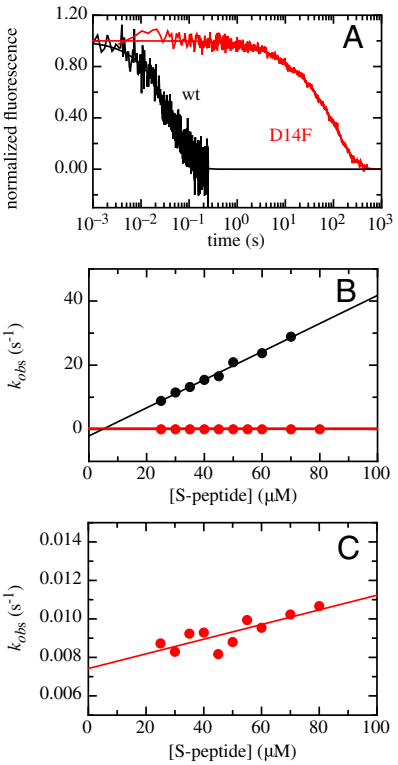

Fig. S4. Kinetics of the association reaction between unfolded S-peptide and folded S-protein. (*A*) Comparison of the wild-type protein (black) and the Asp14Phe variant (red) association reaction monitored by tyrosine fluorescence >305 nm. The concentration of S-protein was 5 μM, the concentration S-peptide was 50 μM in both experiments. (*B*) Pseudo-first-order plot of the association kinetics of the two variants in the presence of increasing S-peptide concentrations and a S-protein concentration of 5 μM. The slope of the plot yields a bimolecular association rate constant of $k_{on} = (4.4 \pm 0.2) \cdot 10^5$ M^{-1} s^{-1} for the wild-type protein and $k_{on} = 38 \pm 9$ M^{-1} s^{-1} for the Asp14Phe variant using $k_{obs} = k_{on} \cdot$ [S-peptide]. Conditions were pH 6.0, 50 mM NaOAc, 100 mM NaCl at 25 °C. (*C*) Zoom of the pseudofirst-order plot for the D14F variant.

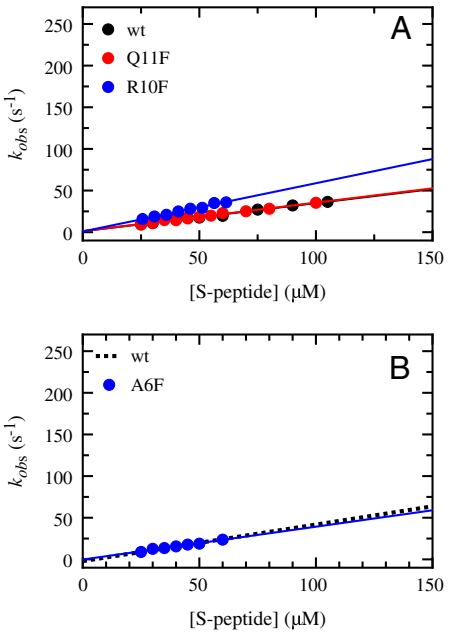

Fig. S5. Effect of various side-chain replacements on the kinetics of association between S-peptide and S-protein under pseudo-first-order conditions at 25 °C (see Fig. 2). For comparison the results for the wild-type S-peptide are shown as dashed line. The resulting k_{on}-values are given in Table 2. Experimental conditions were pH 6.0, 50 mM NaOAc, 100 mM NaCl at 25 °C. The measurements shown in *A* were carried out in the presence of 1% DMSO to increase solubility of the S-peptide variants. Data were analyzed as described in Fig. 2. The presence of DMSO has only minor effects on complex stability and association kinetics of wild-type RNase S (see Table 2).

Table S1. Interactions of the S-peptide C=O groups used for backbone ϕ-value analysis of the S-peptide/S-protein interaction

Position	φ, ψ (C=S)* ($\Delta\Delta G^0$)	C=O interactions	N-H interactions	Packing around C=O
Thr3	favorable	H-bond acceptor from Lys7 amide NH;	none	solvent-exposed
Ala4	favorable	H-bond acceptor from Phe8 amide NH; water-mediated H-bond to Val118 C=O	none	solvent-exposed
Lys7	favorable	H-bond acceptor from Gln11 amide NH Gln11 C^{β}, C^{γ} Lys7 C^{β}, C^{γ}	H-bond donor to Thr3 C=O	close-packing†
Phe8	favorable	H-bond acceptor from His12 amide NH C^{β}, phenyl ring from Phe8. C^{β}, C^{β}-H, imidazole ring from His12	H-bond donor to Ala4 C=O	close-packing
Glu9	favorable	H-bond acceptor from Nle13 amide NH C^{β}, C^{β}-H from Nle13 $N^{\eta 1}$ of Arg33	H-bond donor to Ala5 C=O	close-packing
Arg10	favorable	H-bond acceptor from Arg33 $N^{\eta 1}$ C^{α}, C^{δ} from Arg10 C^{β}, C^{β}-H, C^{δ}, C^{δ}-H from Arg33	H-bond donor to Ala6 C=O;	close-packing
His12	unfavorable	H-bond acceptor from amide NH of Val47 C^{α}-H of Phe46 C^{β} of His12	H-bond donor to Phe8 C=O	close-packing
Ser15	unfavorable	none	none	solvent-exposed

In the region of close-packing the O → S replacement is expected to lead to unfavorable steric effects in the native complex

*The φ,ψ angles from the crystal structure of the all-oxo S-peptide bound to the S-protein are compared to preferred thioxo-peptide bond backbone geometry at this position taken from ref. 1.

†The close-packed hydrophobic pocket involves residues $Val^{47,54,57,108}$, $Ile^{81,106}$, Leu^{51}, Met^{79}, Pro117, and Phe^{120} of the S-protein.

1 Wildemann D, et al. (2007) A nearly isosteric photosensitive amide-backbone substitution allows enzyme activity switching in ribonuclease S. *J Am Chem Soc* 129:4910–4818.

Table S2. Interactions of the S-peptide side chains used for ϕ-value analysis of the S-peptide/S-protein interaction

Position	Side-chain interactions	Area of nonpolar interaction (Å^2) S-peptide + S-protein	Packing
Ala5	C^{γ}, $C^{\delta 2}$ of Leu35	34.2 + 29.0	solvent-exposed
Ala6	none	-	solvent-exposed
Lys7	none	-	solvent-accessible
Phe8	helix-stabilizing interaction with His12; C^{β}, $C^{\delta 1}$ $C^{\varepsilon 1}$, $C^{\varepsilon 2}$, C^{ζ} to Phe46 $C^{\delta 1}$	114.5 + 19.1	close-packing*
Glu9	water-mediated H-bond of $O^{\varepsilon 2}$ to $N^{\varepsilon 2}$ of Gln^{55}; helix-stabilizing salt bridge to His12 in the isolated helix.	-	solvent-accessible
Arg10	Salt bridge with Glu2 COOH $N^{\eta 1}$: H-bond donor to Arg33 C=O; C^{γ}, C^{δ} to His48	34.4 + 28.0	packing
Gln11	side-chain interaction with Leu51 $C^{\delta 1}$, $C^{\delta 2}$	15.0 + 66.2	packing
His12	helix-stabilizing interaction with Phe8. H-bond from $N^{\delta 1}$ to C=O of Thr45 C^{β}, C^{ε} to Val54 $C^{\gamma 1}$ active-site acid	68.1 + 18.6	close-packing
Nle13	C^{δ}, $C^{\varepsilon 1}$ to Val116 $C^{\gamma 2}$	67.1 + 22.3	close-packing
Asp14	C^{β} to Val 118 $C^{\gamma 1}$ and Phe120 C^{β} C^{β} and $O^{\delta 2}$ to Tyr25 C^{ε}	40.2 + 80.0	close-packing

*The close-packed hydrophobic pocket involves residues $Val^{47,54,57,108}$, $Ile^{81,106}$, Leu^{51}, Met^{79}, Pro117, and Phe^{120} of the S-protein.

Table S3. Effect of side-chain replacements on stability and association kinetics of the S-peptide/S-protein complex at pH 6, 50 mM NaCac, 100 mM NaCl, 10 °C

S-peptide	K_{eq} (M^{-1})	$\Delta\Delta G^0$ (kJ/mol)	k_{on} ($M^{-1}\,s^{-1}$)	$\Delta\Delta G^{0\ddagger}$ (kJ/mol)	ϕ-value
WT	$(1.9 \pm 0.1) \cdot 10^7$	-	$(2.0 \pm 0.1) \cdot 10^5$	-	-
WT pH 8.5	$(1.0 \pm 0.1) \cdot 10^8$	−3.9	$(4.9 \pm 0.1) \cdot 10^5$	−2.9	-
A5F	$(1.5 \pm 0.2) \cdot 10^7$	0.6	$(2.2 \pm 0.1) \cdot 10^5$	0.3	n.w.d.
A6F	$(2.8 \pm 0.1) \cdot 10^6$	4.6	$(1.4 \pm 0.1) \cdot 10^5$	0.6	0.14
K7F	$(1.4 \pm 0.1) \cdot 10^7$	0.8	$(3.6 \pm 0.2) \cdot 10^5$	−1.4	<0
F8Y*	$(4.0 \pm 0.3) \cdot 10^4$	14.1	$(8.8 \pm 0.1) \cdot 10^4$	1.9	0.13
F8W	$(7.5 \pm 0.2) \cdot 10^4$	11.7	$(3.8 \pm 0.3) \cdot 10^5$	−2.3	<0
F8Nal	$(5.8 \pm 0.4) \cdot 10^6$	2.9	$(4.6 \pm 0.1) \cdot 10^5$	−2.0	<0
E9Q	$(2.7 \pm 0.3) \cdot 10^7$	−0.8	$(2.7 \pm 0.1) \cdot 10^5$	−0.8	n.w.d.
E9F	$(2.7 \pm 0.3) \cdot 10^7$	−0.8	$(9.1 \pm 0.1) \cdot 10^5$	−3.6	<0
R10F†	$(5.5 \pm 0.5) \cdot 10^6$	3.0	$(2.2 \pm 0.1) \cdot 10^5$	−0.5	<0
Q11F†	$(1.3 \pm 0.1) \cdot 10^7$	1.0	$(1.9 \pm 0.1) \cdot 10^5$	0.1	n.w.d.
H12A	$(3.4 \pm 0.1) \cdot 10^5$	9.5	$(4.1 \pm 0.1) \cdot 10^5$	−1.8	<0
H12F	$(8.7 \pm 0.3) \cdot 10^5$	7.2	$(1.7 \pm 0.1) \cdot 10^6$	−5.1	<0
Nle13A	$(1.2 \pm 0.1) \cdot 10^5$	12.0	$(1.8 \pm 0.1) \cdot 10^5$	0.2	0
Nle13F	$(2.0 \pm 0.1) \cdot 10^6$	5.3	$(3.0 \pm 0.1) \cdot 10^5$	−1.0	<0
D14F	$(6.8 \pm 0.9) \cdot 10^5$	7.9	not determined		-

*Equilibrium constant determined by an activity assay due to the low stability of the complex
†Kinetics measured in the presence of 1% DMSO to increase solubility.